Electronic Supplementary Material (ESI) for Catalysis Science & Technology.

Supporting Information

Simple conversion of earth-abundant coal to high-performance bifunctional oxygen electrode

Xingxing Chen,*[a] Jun Wang,[a] Xinning Huang,[b] Xuefei Zhao,[a]
Bingcai He,[a] Penggao Liu,[c] Tao Wang,*[c] Justus Masa*[d]

[a] Research Group of Functional Materials for New Energy, School of Chemical Engineering, University of Science and Technology Liaoning, Qianshan Middle Road 185, 114051 Anshan, China. E-mail: xingchenstar79@163.com

[b] Engineering Training Center, University of Science and Technology Liaoning, Qianshan Middle Road 185, 114051 Anshan, China

[c] Key Laboratory of Energy Materials Chemistry, Institute of Applied Chemistry, Xinjiang University, Shengli Road 14, 830046 Urumqi, China, E-mail: renbility @163.com

[d] Analytical Chemistry - Center for Electrochemical Sciences (CES), Ruhr-Universität Bochum, Universitätsstr. 150, 44780 Bochum, Germany, E-mail: justus.masa@rub.de

Electrochemical performance of different coal-based carbon materials

In order to evaluate the feasibility of directly modifying natural coal to develop bifunctional oxygen reduction/oxygen evolution catalysts for reversible oxygen electrodes, coal samples from three different locations of the Hailar coal mine (Inner Mongolia), denoted as Hailer 1, Hailer 2 and Hailer 3, were treated at 800°C under ammonia for 2 hours and subsequently investigated for the oxygen reduction reaction (ORR) and the oxygen evolution reaction (OER) in 0.1 M KOH. Table S1 shows the results of proximate analysis of different pristine coals. Figure S1 shows the RRDE voltammograms for the ORR and the corresponding ring current due to H_2O_2 production, as well as linear sweep voltammograms of the OER on the different coal-based carbon materials. The Hailar 1 sample, denoted in the main text as MC-X, where X = temperature of thermal treatment under ammonia, showed the best electrocatalytic performance for both the ORR and the OER. Hailar 1, was therefore selected for further in-depth characterization and optimization of the thermal treatment.

Table S1. Proximate analysis of coal samples from three different locations of the Hailar coal mine.

Sample	**M_{ad}[a]/%**	**A_{ad}[b]/%**	**V_{ad}[d]/%**	**V_{daf}[d]/%**	**FC_{ad}[e]/%**
Hailar1	30.87	10.30	26.46	---	32.37
Hailar2	14.39	9.95	35.42	39.33	40.24
Hailar3	14.88	12.12	33.98	---	39.02

[a] M_{ad}: moisture, [b] A_{ad}: ash, [c] V_{ad}: volatile matter, [d] V_{daf}: volatile matter, [e] FC_{ad}: fixed carbon (All the quantities are on a dry weight basis).

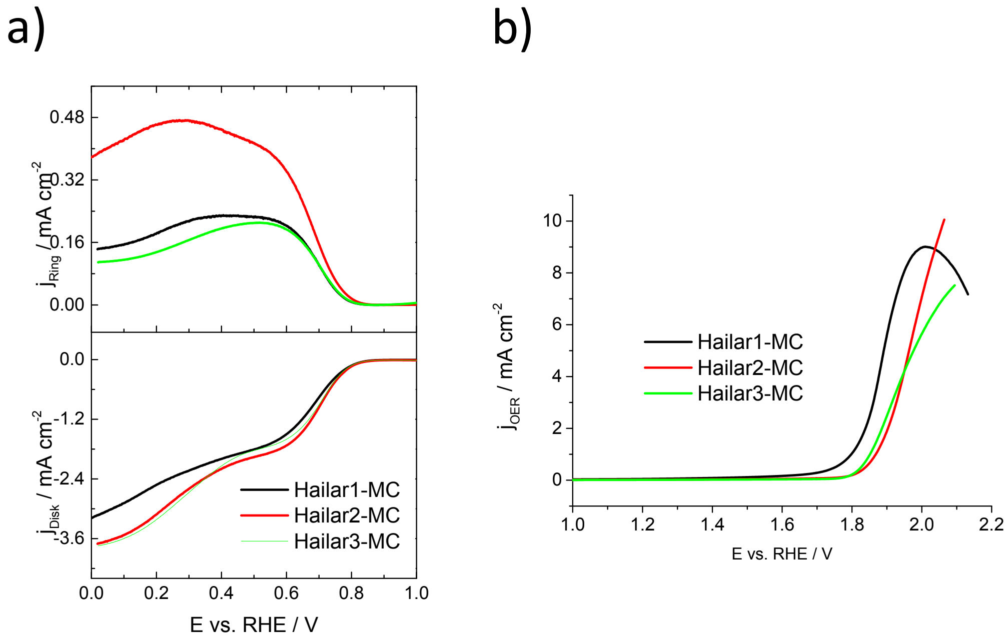

Figure S1. a) RRDE voltammograms showing the ORR performance of different samples of coal from the Hailar coal mine (Inner Mongolia), Hailar 1, Hailar 2 and Hailar 3, and their respective H_2O_2 production, and b) corresponding linear sweep voltammograms showing the OER the samples in O_2-saturated 0.1 M NaOH. The samples were treated at 800^{o}C for two hours under ammonia flow.

Characterization of the MC-1050-Ar sample using XRD, RAMAN and XPS

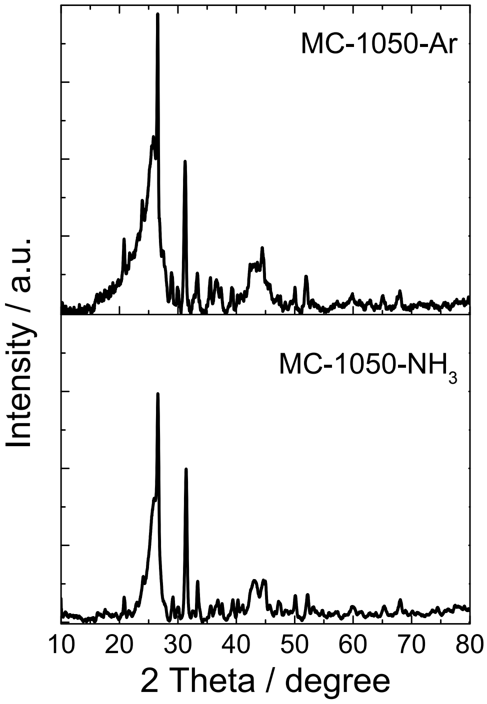

Figure S2. XRD spectra of MC-1050 pyrolyzed in the presence and absence of NH$_3$.

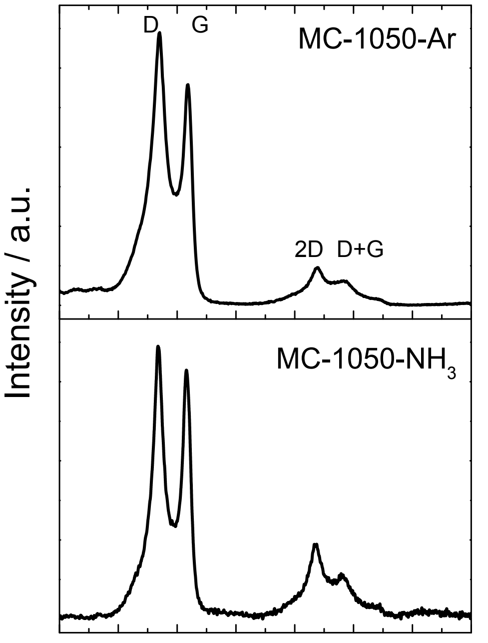

Figure S3. Raman spectra of MC-1050 pyrolyzed in the presence and absence of NH$_3$.

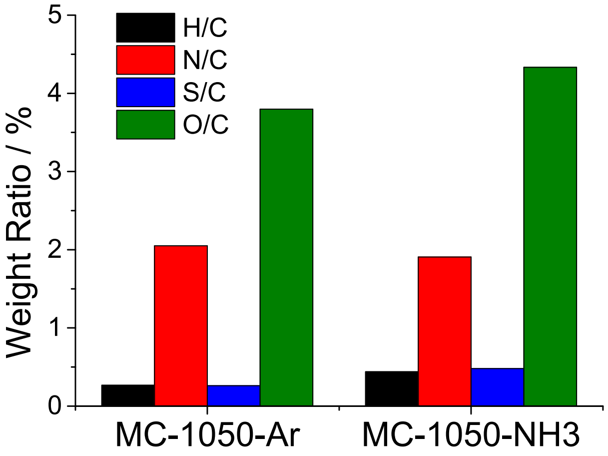

Figure S4. Elemental analysis - relative weight ratio of a) H/C, b) O/C, c) N/C, d) S/C in MC-1050 pyrolyzed in the presence and absence of NH$_3$.

Table S2. Elemental analysis of the original coal (OC) and MC catalysts.

Sample	C%	H%	O%	N%	S%	Ash%
MC-1100-Ar	78.99	0.21	3.00	1.62	0.21	15.97
MC-1100-NH$_3$	75.54	0.33	3.27	1.44	0.36	19.06

* The ash content was obtained by subtracting the other elements (C, H, O, N, S) (wt.% dry basis) from total.

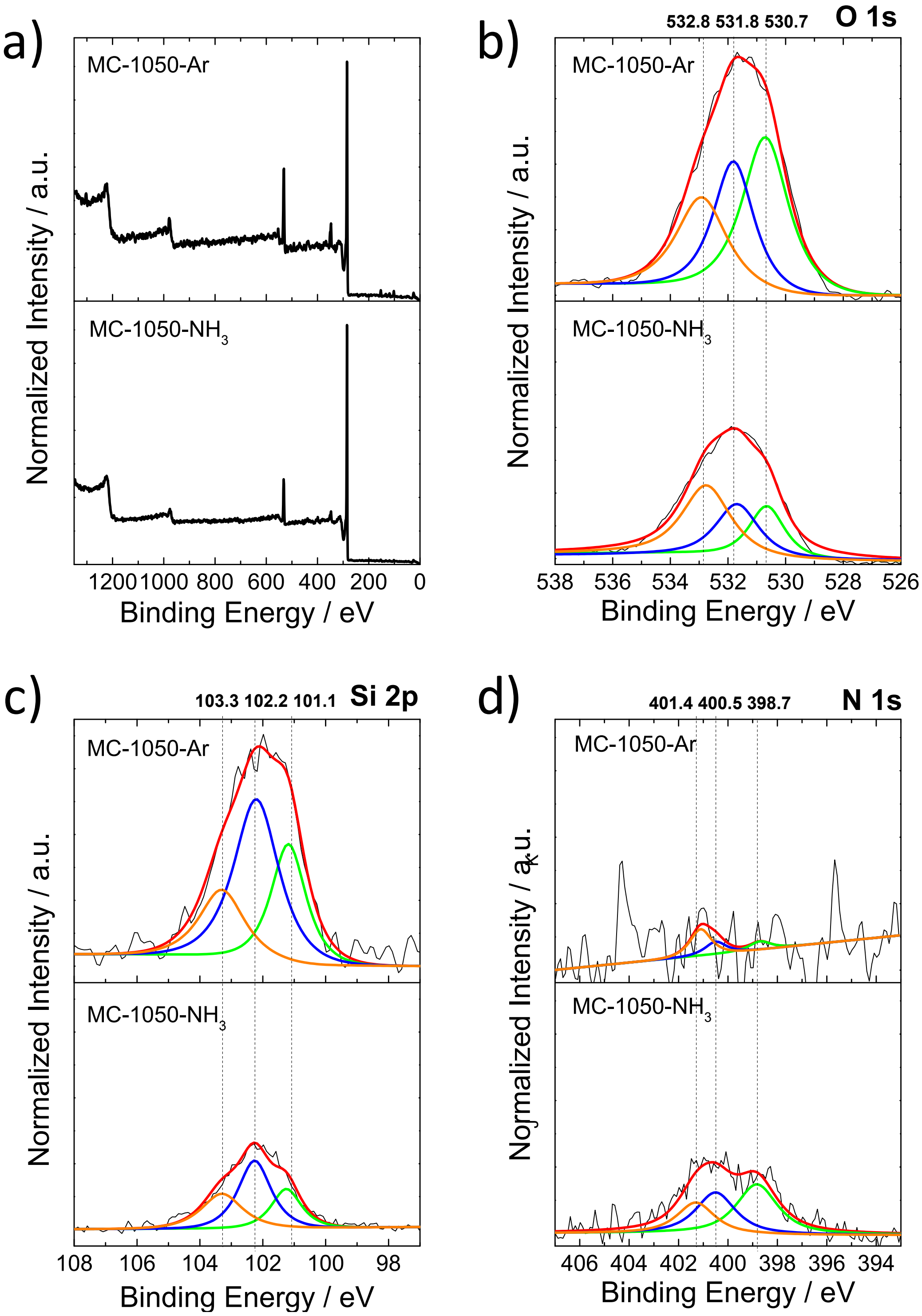

Figure S5. a) XP survey spectra, b) XP O 1s, c) Si 2p and d) N 1s spectra of MC-1050 pyrolyzed in the presence and absence of NH_3. (O^{2-}: 530.7 eV, C=O: 531.8 eV, C-O: 532.8 eV; Si-C: 101.1 eV, C-Si-O: 102.2 eV, SiO_2: 103.3 eV; Pyridinic N: 398.7 eV, Pyrrolic N: 400.5 eV, Quaternary N: 401.4 eV)

Table S3. Relative concentration of different oxygen, nitrogen and silicon contributions obtained by deconvolution of XP O 1s, N 1s and Si 2p spectra, respectively.

Surface Functional Groups		**MC-1100-Ar**	**MC-1100-NH$_3$**
O 1s	O^{2-}%	42.8	22.3
	C=O%	30.8	38.9
	C-O%	26.4	38.8
N 1s	Pyridinic N%	17.5	42.6
	Pyrrolic N%	26.3	33.5
	Graphitic N%	56.2	23.8
Si 2p	Si-C%	29.1	20.0
	C-Si-O%	50.3	53.3
	SiO_2%	20.6	26.7

The bifunctional activity of state-of-the-art bifunctional catalysts

Table S4. The bifunctional activity of state-of-the-art carbon based bifunctional ORR/OER catalysts, including transition metal containing composites and metal-free nanocarbon materials.

Sample	E_{ORR} [V] @ -1 mA cm^{-2}	E_{OER} [V] @ 10 mA cm^{-2}	ΔE = E_{OER}-E_{ORR} [V]	Catalyst Loading [mg cm^{-2}]	Reference
MC-1100	0.81	1.78	0.97	0.21	This work
Mn_xO_y/NC	0.81	1.68	0.87	0.21	[1]
Ni_xO_y/NC	0.71	1.64	0.93	0.21	[1]
Co_xO_y/NC	0.80	1.66	0.86	0.21	[1]
NPMC1000	0.94	1.93	0.99	0.15	[2]
NGM	0.89	1.67	0.78	0.25	[3]
GM	0.83	1.64	0.81	0.25	[3]
NG	0.88	$>$1.98	$>$1.10	0.25	[3]
NGSH	0.88	1.63	0.75	0.25	[4]
GSH	0.85	1.74	0.89	0.25	[4]

Detection of oxygen evolution during the OER

In order to confirm that the current measured during anodic polarization of the MC-1100 modified electrode was from the oxidation of water to oxygen, a Clark-type oxygen sensor (Leici JPBJ-608, INESA Scientific Instrument Co. Ltd, China), was used to detect oxygen production during the OER. Figure S2 presents the concentration of dissolved oxygen with time during constant electrode polarization at 1.77 V (versus RHE). As can be seen, the concentration of dissolved oxygen increased with time thus confirming the production of oxygen under these conditions.

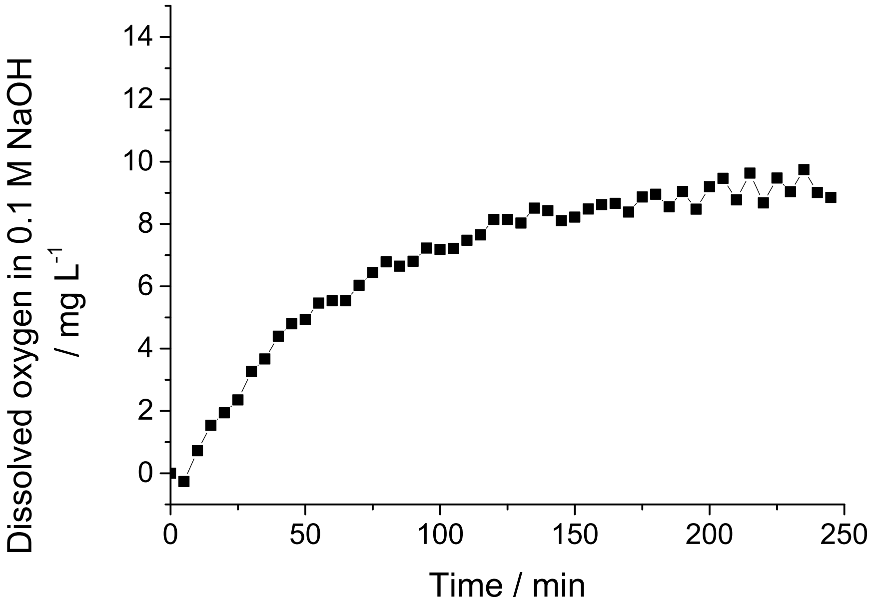

Figure S6. The concentration of dissolved O_2 with time in 0.1 M NaOH during the OER at a graphite electrode modified with the MC-1100 catalyst. The electrode was polarized at a constant potential of 1.77 V vs. RHE, and the catalyst loading was 0.210 mg cm^{-2}.

Determination of Faraday Efficiency during oxygen evolution

The Faraday efficiency during the OER was determined by means of a rotating ring-disk electrode (RRDE) in Ar-saturated 0.1 M NaOH. The sample was loaded on the glassy carbon disk electrode, which was polarized at a constant potential of 1.77 V vs. RHE for OER, while the Pt-ring was continuously held at 0.27 V vs. RHE, where oxygen reduction is expected to proceed at a rate limited by diffusion. The FE was calculated from the equation of FE = $I_{ring}/(CE*I_{disk})$, where I_{ring} is the ring current, I_{disk} is the disk current, and CE is the collection efficiency of the ring. The CE of the ring was determined for the individual catalyst films using a 5.0 mM solution of $K_3[Fe(CN)_6]$ in 0.1 M NaOH. For the MC-1100 film of the data in Figure S3, the CE was 0.24 (Figure S3b).

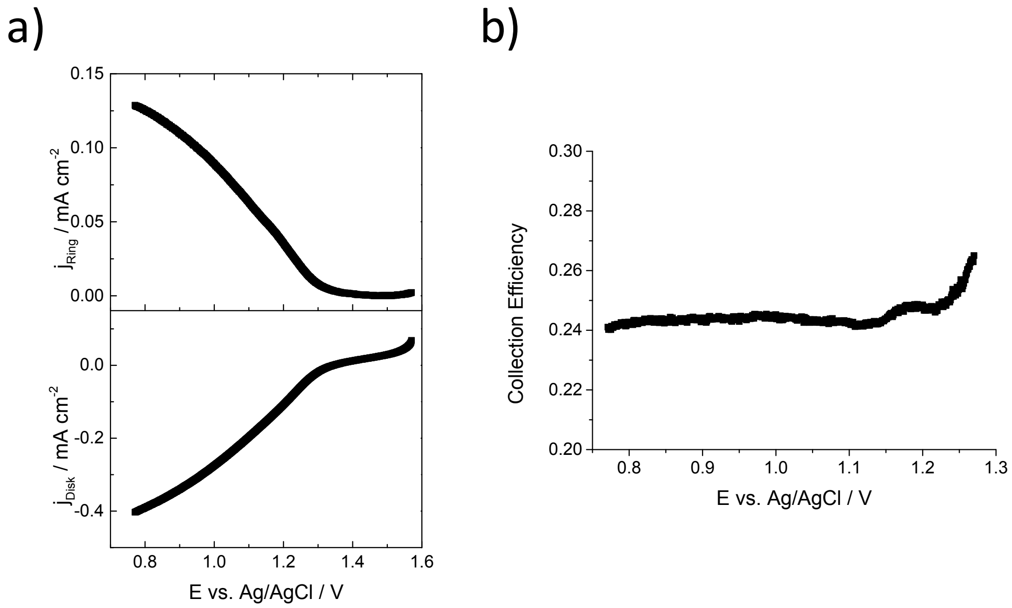

Figure S7. Determination of the collection efficiency of the RRDE with the disk modified with a MC-1100 catalyst film in Ar-saturated 5mM $K_3[Fe(CN)_6]$ in 0.1 M NaOH solution. The glassy carbon-disk supported MC-1100 was polarized from 1.57 to 0.77 V, while the Pt-ring was held at 1.37 V vs. RHE.

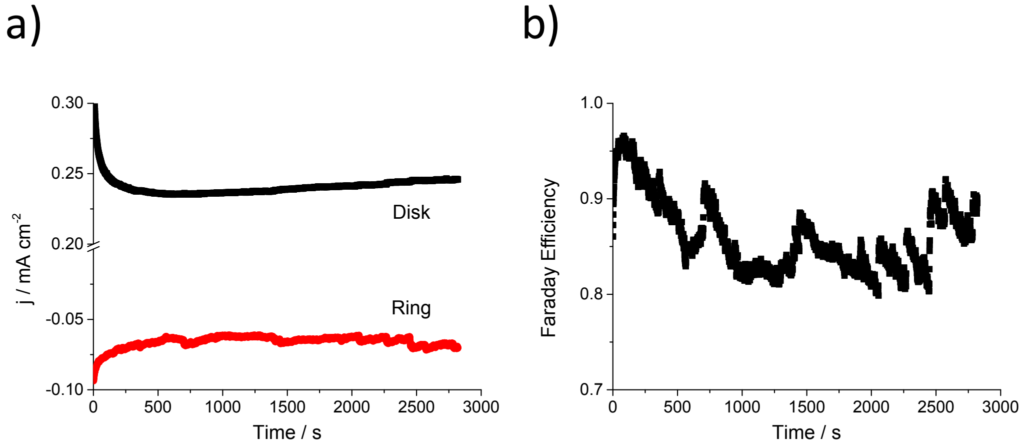

Figure S8. Faraday efficiency measurement of oxygen evolution catalyzed by MC-1100 using RRDE voltammetry in Ar-saturated 0.1 M NaOH. The glassy carbon-disk supported MC-1100 was polarized at 1.77 V (OER takes places), while the Pt-ring was held at 0.27 V vs. RHE (ORR takes places).

The FE for oxygen evolution catalyzed by MC-1100 was initially 97 %, but decreased gradually to -about 80%. As can be seen from Figure S4b, the ORR current at the Pt ring exhibited a period decrease and increase, which is associated with bubble accumulation, growth and departure. This phenomenon affects oxygen transport from the disk to the ring, manifesting into an apparently lower Faraday efficiency. The result therefore indicates that most of the current is due to the evolution. Nonetheless, competing parasitic reactions, for example, the oxidation of carbon, cannot be completely excluded.

References

1 J. Masa, W. Xia, I. Sinev, A. Q. Zhao, Z. Y. Sun, S. Gruetzke, P. Weide, M. Muhler and W. Schuhmann, *Angew. Chem. Int. Ed.*, 2014, **53**, 8508.

2 J. Zhang, Z. Zhao, Z. Xia and L. Dai, *Nat. Nanotechnol.*, 2015, **10**, 444.

3 C. Tang. H. F. Wang, X. Chen, B. Q. Li, T. Z. Hou, B. S. Zhang, Q. Zhang, M. M. Titirici and F. Wei, *Adv. Mater*., 2016, **28**, 6845.

4 D. S. Yu, X. Y. Kong, J. Q. Huang, Q. Zhang and F. Wei, *Small*, 2014, **10**, 2251.